Available online at www.sciencedirect.com
SCIENCE DIRECT®
Journal of the Mechanics and Physics of Solids
54 (2006) 561–587
JOURNAL OF THE MECHANICS AND PHYSICS OF SOLIDS
www.elsevier.com/locate/jmps

A non-singular continuum theory of dislocations

Wei Cai[a,*], Athanasios Arsenlis[b], Christopher R. Weinberger[a], Vasily V. Bulatov[b]

[a]*Department of Mechanical Engineering, Stanford University, Stanford, CA 94305-4040, USA*
[b]*Lawrence Livermore National Laboratory, Livermore, CA 94550, USA*

Received 21 April 2005; received in revised form 22 September 2005; accepted 29 September 2005

Abstract

We develop a non-singular, self-consistent framework for computing the stress field and the total elastic energy of a general dislocation microstructure. The expressions are self-consistent in that the driving force defined as the negative derivative of the total energy with respect to the dislocation position, is equal to the force produced by stress, through the Peach–Koehler formula. The singularity intrinsic to the classical continuum theory is removed here by spreading the Burgers vector isotropically about every point on the dislocation line using a spreading function characterized by a single parameter a, the spreading radius. A particular form of the spreading function chosen here leads to simple analytic formulations for stress produced by straight dislocation segments, segment self and interaction energies, and forces on the segments. For any value $a>0$, the total energy and the stress remain finite everywhere, including on the dislocation lines themselves. Furthermore, the well-known singular expressions are recovered for $a=0$. The value of the spreading radius a can be selected for numerical convenience, to reduce the stiffness of the dislocation equations of motion. Alternatively, a can be chosen to match the atomistic and continuum energies of dislocation configurations.

Keywords: Dislocation; Self-force; Singularity; Spreading dislocation core

*Corresponding author. Tel.: +1 6507361671; fax: +1 6507231778.
E-mail address: caiwei@stanford.edu (W. Cai).

0022-5096/$ - see front matter © 2005 Elsevier Ltd. All rights reserved.
doi:10.1016/j.jmps.2005.09.005

1. Introduction

Dislocations are the primary carriers of crystal plasticity and their collective dynamics define material's response to a variety of loading conditions, e.g. in yield, creep or fatigue. Developed over the past two decades, Dislocation Dynamics (DD) is a direct approach that attempts to simulate the aggregate behavior of large dislocation ensembles and holds considerable promise for uncovering the microscopic origins of crystal strength (Devincre and Kubin, 1997; Schwarz, 1999; Ghoniem and Sun, 1999; Cai et al., 2004a; Bulatov et al., 2004). However, in the development of this new methodology, several issues remain unresolved. This contribution addresses and solves the long-standing problem of singularities intrinsic to the classical continuum theory of dislocations. The singular solutions of the continuum theory are analytical and simple, at least for an important case of elastic isotropy. However, the energy and forces can be infinite unless some truncation scheme is applied to avoid the singularities.

Non-singular treatments of dislocations have been the focus of several theoretical studies since the 1960s. Self-consistency in terms of dislocation theory is achieved when forces on the dislocations computed two ways are the same. The first way to compute the force is to take the negative derivative of the elastic energy with respect to the dislocation position. The second way is to use the Peach–Koehler formula relating the force to local stress. Various modifications of the linear isotropic elastic theory have been considered as possible solutions. A heuristic non-singular approach was first proposed by Brown (1964) in which the driving force was related to the average stress evaluated at two points on either side of the dislocation line. Later, Gavazza and Barnett (1976) showed that Brown's recipe lacked consistency and identified a set of correction terms needed to make it self-consistent. In the Gavazza–Barnett approach, only the elastic energy stored in the material outside a tube region surrounding the dislocation line was included in the driving force calculation. This solution was later used for DD simulations (Schwarz, 1999). Unfortunately, consistency of this elegant solution has been rigorously demonstrated only in 2D, i.e. for in-plane components of force on a planar dislocation loop. And while the Gavazza–Barnett solution provided an expression for the derivatives of the elastic energy stored in a dislocation network, it did not provide an explicit expression for the elastic energy itself.

Here we propose a non-singular and self-consistent treatment applicable to an arbitrary dislocation arrangement that satisfies the following four conditions.

(1) Our approach provides explicit non-singular expressions for the total elastic energy and stress field of an arbitrary dislocation structure. In the case of isotropic elasticity, the non-singular solutions are analytic and (nearly) as simple as the classical singular solutions.
(2) The approach is self-consistent in that the force on a dislocation segment defined as the negative derivative of energy with respect to the segment position, is equal to the force obtained by integrating the stress field along the segment (by the Peach–Koehler formula).
(3) The solution can be used for straight segments connected at an arbitrary angle and converges for general curvilinear geometries in the limit when the segment size becomes infinitesimally small.
(4) The solution has a clear connection to the more fundamental, atomistic models of dislocations.

None of the previous treatments has fulfilled all four conditions listed above. The first two conditions point to the desirable mathematical properties that have been sought after in previous investigations. The third condition ensures that the new solutions are robust and usable in the DD simulations where the numerical convergence is all-important. Finally, the fourth condition means that the modification introduced to transform the classical singular theory into a non-singular theory, allows a clear physical interpretation.

The modification we propose is to distribute the Burgers vector about every point on the line: the line now becomes the locus of the centers of the Burgers vector distributions. Our idea is to find a specific Burgers vector distribution such that it yields analytical expressions that are as close as possible to the classical expressions derived within the singular theory. This proposed solution is conceptually similar to the Peierls–Nabarro model (Peierls, 1940; Nabarro, 1947) and to the standard core model (Lothe, 1992) of dislocations, in which the Burgers vector is spread out in the glide planes. The difference is that in our approach the Burgers vector is not distributed over a plane but in all directions about every point on the line.

The discussion is organized as follows. Section 2 details the issues associated with the classical singular solutions for the dislocation energies and stress fields in elastically isotropic solids. Section 3 reviews the previous non-singular treatments and discusses their advantages and drawbacks. Sections 4 and 5 develop our new isotropic model while Section 6 presents numerical results demonstrating its self-consistency and convergence properties. Section 7 compares our model with the Gavazza and Barnett (1976) model and demonstrates their relationship. Finally, Section 8 gives a summary and discusses new opportunities this approach offers to dislocation modeling.

2. Problem formulation

The Peach–Koehler formula (Hirth and Lothe, 1982) expresses the driving force (per unit length) $\mathbf{f}$ that local stress $\boldsymbol{\sigma}$ exerts on a dislocation line,

$$\mathbf{f} = (\boldsymbol{\sigma} \cdot \mathbf{b}) \times \boldsymbol{\xi}, \tag{1}$$

where $\mathbf{b}$ is the dislocation Burgers vector and $\boldsymbol{\xi}$ is the local tangent (unit vector) of the dislocation line. For example, if $\boldsymbol{\sigma}$ is stress at a point on a dislocation line due to externally applied tractions, then $\mathbf{f}$ is the force per unit length on this point due to the tractions. In a DD simulation, forces caused by external tractions combine with forces induced by internal stress produced by the dislocation microstructure.

In a homogenous infinite linear elastic solid, the (internal) stress field of a dislocation loop can be expressed in terms of a contour integral along the loop (Mura, 1982),

$$\sigma_{ij}(\mathbf{x}) = C_{ijkl} \oint_C \varepsilon_{lnh} C_{pqmn} G_{kp,q}(\mathbf{x} - \mathbf{x}') b_m \, \mathrm{d}x'_h, \tag{2}$$

where C_{ijkl} is the elastic stiffness tensor, $G_{kp,q} = \partial G_{kp}/\partial x_q$. Here, $G_{kp}(\mathbf{x} - \mathbf{x}')$ is the Green's function defined as the displacement in x_k-direction at point $\mathbf{x}$ in response to a unit point force in x_p-direction applied at point $\mathbf{x}'$. In an isotropic elastic solid with the shear modulus μ and the Poisson's ratio ν, the Green's function takes the following simple form:

$$G_{ij}(\mathbf{x} - \mathbf{x}') = \frac{1}{8\pi\mu}\left[\delta_{ij}\partial_p\partial_p R - \frac{1}{2(1-\nu)}\partial_i\partial_j R\right], \tag{3}$$

where $\partial_i \equiv \partial/\partial x_i$ and $R = \|\mathbf{x} - \mathbf{x}'\|$. The stress field of a dislocation loop can thus be expressed as

$$\sigma_{\alpha\beta}(\mathbf{x}) = \frac{\mu}{8\pi} \oint_C \partial_i \partial_p \partial_p R [b_m \varepsilon_{im\alpha} \, \mathrm{d}x'_\beta + b_m \varepsilon_{im\beta} \, \mathrm{d}x'_\alpha] + \frac{\mu}{4\pi(1-\nu)} \oint_C b_m \varepsilon_{imk} (\partial_i \partial_\alpha \partial_\beta R - \delta_{\alpha\beta} \partial_i \partial_p \partial_p R) \, \mathrm{d}x'_k. \tag{4}$$

As the field point $\mathbf{x}$ approaches the source point $\mathbf{x}'$ in the above integral, R approaches zero and some (if not all) components of the stress tensor diverge. Therefore, the self-force of a dislocation line, i.e. the force due to its own stress field, diverges too. This singular behavior is an artifact traced to the unrealistic assumption that the Burgers vector distribution is a delta function. In the atomistic models that provide more realistic description of the dislocation core, this problem never arises.

A similar divergent behavior occurs in the expressions for the elastic energy of dislocations. There are two equivalent ways to express the total elastic energy, both leading to infinity. On way is to integrate the elastic energy density over the entire volume, i.e.,

$$E = \frac{1}{2} \int \mathrm{d}^3\mathbf{x} \, S_{ijkl} \sigma_{ij}(\mathbf{x}) \sigma_{kl}(\mathbf{x}), \tag{5}$$

where $S = C^{-1}$ is the elastic compliance tensor. Because the stress field $\sigma_{ij}(\mathbf{x})$ has $1/R$ singularity on the dislocation line itself, the volume integral obviously diverges. Another, alternative, expression for the elastic energy is obtained by transforming the volume integral into a double line integral (de Wit, 1976a, b)

$$E = -\frac{\mu}{8\pi} \oint_C \oint_C \partial_k \partial_k R b_i b'_j \, \mathrm{d}x_i \, \mathrm{d}x'_j - \frac{\mu}{4\pi(1-\nu)} \oint_C \oint_C \partial_i \partial_j R \, b_i b'_j \, \mathrm{d}x_k \, \mathrm{d}x'_k + \frac{\mu}{4\pi(1-\nu)} \left[\oint_C \oint_C \partial_k \partial_k R \, b_i b'_i \, \mathrm{d}x_j \, \mathrm{d}x'_j - \nu \oint_C \oint_C \partial_k \partial_k R \, b_i b'_j \, \mathrm{d}x_j \, \mathrm{d}x'_i \right]. \tag{6}$$

The total integrand above can be identified with the interaction energy between two differential dislocation segments $\mathrm{d}\mathbf{x}$ and $\mathrm{d}\mathbf{x}'$. Again, this integral is unbounded because the integrand diverges as $\mathbf{x}$ and $\mathbf{x}'$ approach each other ($R \to 0$). The divergent behaviors discussed here can result in ill-defined numerical procedures for computing the energies and forces associated with dislocations.

3. Earlier attempts to remove the singularities

In this section, we review several earlier attempts to remove (or avoid) the singularities in the continuum theory of dislocations. No consideration will be given to the previous work on non-local or gradient elasticity (Gutkin and Aifantis, 1996, 1997) and finite-strain elasticity (Fedelich, 2004). Rather, we will discuss only the treatments closely related to the objectives of this particular study.

Approach I. Since 1960s, several schemes have been proposed to remove the singularities from dislocation theory and to define a finite self-force on dislocations. In Hirth and Lothe (1982), a cut-off radius ρ is introduced to regularize the elastic energy of a dislocation loop. In the double line integral for the elastic energy (similar to Eq. (6)) the following *regularization convention* is used. *The integrand is set to zero whenever the distance between the differential segments* $\mathrm{d}\mathbf{x}$ *and* $\mathrm{d}\mathbf{x}'$ *becomes less than* ρ. Following this convention, elastic

energy of an arbitrary dislocation loop becomes finite. In principle, the forces can be defined self-consistently as the negative derivatives of, now finite, energy with respect to appropriate dislocation configuration variables. In practice, self-consistency of this approach has not been enforced.

In numerical calculations, dislocations are often represented by interconnected straight segments. The elastic energy, E, of so-discretized dislocations is partitioned into two sums: a sum of the segment self-energies W_i^{s} and a sum of the interaction energies W_{ij}^{int} of segments pairs (i and j) (Cai, 2001)

$$E = \sum_i W_i^{\mathrm{s}} + \sum_{i<j} W_{ij}^{\mathrm{int}}. \tag{7}$$

This standard partitioning of the elastic energy makes the above *regularization convention* difficult to implement rigorously. This is because an analytical expression for W_{ij}^{int} is available only when the above convention is ignored, i.e. all points on segments i and j are included in the integral. This inconsistency does not appear when the segments are well separated, so that even their closest distance is larger than ρ. However, when this is not the case, e.g. when two segments share a common node (Fig. 1), the analytical expressions do not faithfully account for the regularization convention leading to inconsistent implementations.

Another artifact of the above regularization approach is the following. Historically several alternative expressions for the line integral of the dislocation energy, such as Eq. (6), have been derived (Blin, 1995; de Wit, 1960, 1967a, b) in which the forms of the integrand differ but the differences vanish when the integrals are evaluated over an entire dislocation loop. Unfortunately, since the *regularization convention* described above effectively cuts open the (otherwise complete) dislocation loop, it was found that different integrands produce different self-energies of a dislocation loop, even when the same cut-off parameter ρ is used (LeSar, 2004). To remedy this inconsistency, it was proposed to use a cut-off parameter ρ that depends both on the dislocation character angle and on the specific form of the integrand used (Lothe and Hirth, 2005).

Approach II. Another approach is offered by Brown (1964) who averts the singularity by defining the stress as an average of stress evaluated at two points on the opposite side of

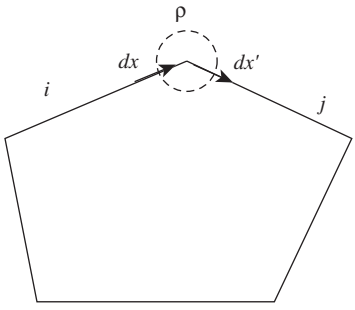

Fig. 1. To remove singularities from the elastic energy of a dislocation loop, one convention is to ignore the interaction between differential segments whose distance from each other is less than ρ. This removes part of the interaction energy between two neighboring segments i and j sharing a node. Unfortunately, this "distance cut-off" convention has not been enforced consistently owing to the lack of analytic expressions for the interaction energy between two hinged segments with "excluded" length (Hirth and Lothe, 1982).

and at a short distance ρ away from the line (Fig. 2). In this convention, the glide component of the force $\mathbf{f}^{\mathrm{B}}$ on the dislocation at point $\mathbf{P}$ is defined as

$$f_i^{\mathrm{B}}(\mathbf{P})m_i \equiv -\tfrac{1}{2}b_i n_j\{\sigma_{ij}^{\mathrm{L}}(\mathbf{P}+\rho\mathbf{m}) + \sigma_{ij}^{\mathrm{L}}(\mathbf{P}-\rho\mathbf{m})\}, \tag{8}$$

where

$$\mathbf{n} = \frac{\mathbf{b}\times\boldsymbol{\xi}}{\|\mathbf{b}\times\boldsymbol{\xi}\|}, \tag{9}$$

$$\mathbf{m} = \boldsymbol{\xi}\times\mathbf{n}. \tag{10}$$

Following this definition, the contribution of a straight dislocation to its self-force is zero (Fig. 2(a)). For curved dislocations (Fig. 2(b)), Eq. (8) gives rise to a non-zero self-force.

One limitation of Brown's approach is that it defines only the *glide* component of the Peach–Koehler force, i.e. the projection of the total force on the glide direction $\mathbf{m}$. At the same time, the remaining component that induces non-conservative *climb* motion remains undefined. Furthermore, as was later shown by Gavazza and Barnett (1976), Brown's recipe is not self-consistent in that $\mathbf{f}^{\mathrm{B}}$ is not the negative derivative of a dislocation energy function. Gavazza and Barnett (1976) also showed that corrections to Brown's force equation could be added to make it self-consistent.

Approach III. Gavazza and Barnett (1976) derived the following expression, $\mathbf{f}^{\mathrm{GB}}$, for the force on a dislocation line:

$$f_i^{\mathrm{GB}}(\mathbf{P})m_i \equiv f_i^{\mathrm{B}}(\mathbf{P})m_i + \frac{1}{r}\left\{E(\alpha) - \left[F(\alpha) + \frac{\partial^2 F}{\partial\alpha^2}\right]\right\}, \tag{11}$$

where r is the local radius of curvature at point $\mathbf{P}$, E is an energy pre-factor of an infinite straight dislocation with tangent $\boldsymbol{\xi}$, F is a "tube integral" around the same dislocation. Both E and F are functions of the angle α between $\boldsymbol{\xi}$ and a datum (Fig. 2(b)). They arrived at this expression by finding the total elastic energy of a dislocation loop based on a volume integral similar to Eq. (5), but excluding from this integral a tubular region around the loop with radius ρ. The force $\mathbf{f}^{\mathrm{GB}}$ on a dislocation line is then determined by differentiating the energy with respect to the line position.

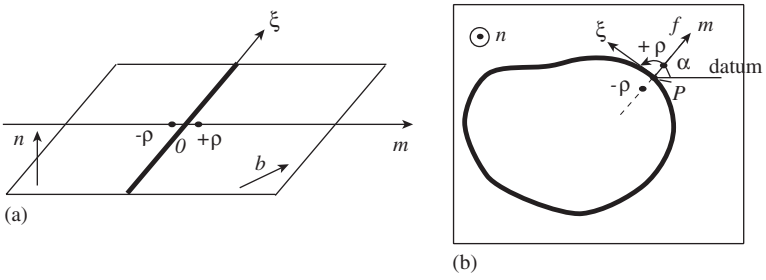

Fig. 2. (a) Because the stress field is anti-symmetric around an infinite straight dislocation, the average of stress taken at two points at a distances $\pm\rho$ from the line is zero. Consequently, the straight dislocation produces no self-force in Brown's approach. Here $\boldsymbol{\xi}$ is the line direction, $\mathbf{n}$ is the glide plane normal, $\mathbf{m}$ is a unit vector perpendicular to $\boldsymbol{\xi}$ and $\mathbf{n}$, and $\mathbf{b}$ is the Burgers vector. (b) $\mathbf{P}$ is a point on a dislocation loop on a plane with normal vector $\mathbf{n}$. $\boldsymbol{\xi}$ is the local tangent direction shown here at an angle α with respect to a datum. $\mathbf{m}$ is orthogonal to both $\mathbf{n}$ and $\boldsymbol{\xi}$. In Brown (1964), the self-force $\mathbf{f}$ at point $\mathbf{P}$ is computed by applying the Peach–Koehler formula on the averaged stress taken at two points $\mathbf{P}\pm\rho\mathbf{m}$.

Similar to Brown's, Gavazza–Barnett approach provides expressions only for the glide component of force. Another common limitation is that validity of either method for non-planar dislocation configurations has not been demonstrated. In principle, both methods require the dislocation line to be smooth, so that vectors $\boldsymbol{\xi}$ and $\mathbf{m}$ can be defined on every point P along the line. Furthermore, the correction term of Gavazza–Barnett is proportional to $1/r$, which makes it difficult to deal with sharp corners where the radius of line curvature is zero.[1]

Approach IV. Another well-known approach is due to Lothe (1992), who removes (or weakens) the singularity by spreading the dislocation core over a finite width on the glide plane. This is not unlike the classical Peierls–Nabarro model (Peierls, 1940; Nabarro, 1947) in which the spreading function is determined self-consistently, by the balance between the elastic energy in the bulk and the non-linear interface energy on the glide plane. While the Peierls–Nabarro model provided analytical expressions for the stress field and the energy of an infinite straight dislocation, it did not offer analytical expressions for the energy or forces of the generally curved dislocation lines. Lothe simplifies the Burgers vector distribution within the core by spreading it uniformly in a plane over a fixed width d: this is commonly referred to as the *standard reference* core. Lothe shows that the glide force, $\mathbf{f}^{\mathrm{L}}$, on a dislocation line with a standard core of width $d = \rho$ reduces to

$$f_i^{\mathrm{L}}(\mathbf{P})m_i \equiv f_i^{\mathrm{B}}(\mathbf{P})m_i + \frac{1}{r}E(\alpha), \tag{12}$$

where $(1/r)E(\alpha)$ is the same function as in the Gavazza and Barnett expression (Eq. (11)).

The stress and energy of dislocations with a standard core can be obtained by convoluting the classical singular expressions with the (uniform) spreading function. For example, for an infinite straight screw dislocation stretching out along z-axis, the singular expression for σ_{yz} is

$$\sigma_{yz} = \frac{\mu b}{2\pi x}. \tag{13}$$

When the same Burgers vector is spread over the interval $x \in [-d/2, d/2]$, the stress field becomes

$$\sigma_{yz} = \begin{cases} \dfrac{\mu b}{2\pi d}\ln\left(\dfrac{x + d/2}{x - d/2}\right), & x > d/2, \\ \dfrac{\mu b}{2\pi d}\ln\left(\dfrac{d/2 + x}{d/2 - x}\right), & -d/2 < x < d/2. \end{cases} \tag{14}$$

The stress field now has a weaker, logarithmic singularity, but it is integrable so that the total elastic energy remains finite. While Lothe's is an appealing and simple idea, the resulting expressions for the stress field and elastic energy are much more complicated than the original singular equations and difficult to use for generally curved dislocations.

[1] Although this last point may seem unimportant, it presents a significant limitation because sharp corners on dislocations appear in a number of physically important situations, e.g. in cross-slip nodes or junction nodes joining together three or more dislocation lines.

4. Isotropic dislocation core distribution

As discussed in the preceding section, both simplicity and singularity of the classical theory result from an unphysical yet mathematically convenient description of the dislocation core in which the distribution of the Burgers vector is described by a delta function. As noted by Lothe (1992), use of distributions other than the delta-function leads to solutions that are non-singular but considerably more complicated than their singular counterparts. The purpose of this work is to find a Burgers vector distribution that removes the singularities but retains the analytical nature of the classical theory and supplies simple closed form expressions for the stress field and the elastic energy of general dislocation configurations.

To facilitate our discussion, let us first rewrite Eqs. (4) and (6) in the following compact forms:

$$\sigma_{\alpha\beta}(\mathbf{x}) = \oint_C A_{\alpha\beta ijklm}\partial_i\partial_j\partial_k R(\mathbf{x}-\mathbf{x}')b_m \,\mathrm{d}x'_l, \tag{15}$$

$$E = \oint_C \oint_C B_{ijklmn}\partial_i\partial_j R(\mathbf{x}-\mathbf{x}')b_m b'_n \,\mathrm{d}x_k \,\mathrm{d}x'_l, \tag{16}$$

where $A_{\alpha\beta ijklm}$ and B_{ijklmn} are defined by comparing Eqs. (4) and (6) to Eqs. (15) and (16), respectively.

The next step is to introduce a Burgers vector density function $\mathbf{g}(\mathbf{x})$ that removes the dislocation singularity by spreading its Burgers vector $\mathbf{b}$ around every point on the line as follows:

$$\mathbf{b} = \int \mathbf{g}(\mathbf{x})\,\mathrm{d}^3\mathbf{x}. \tag{17}$$

This normalization condition ensures that both the magnitude and the direction of the Burgers vector remain unchanged. For a dislocation loop whose Burgers vector is spread out according to $\mathbf{g}(\mathbf{x})$, its stress field and elastic energy are

$$\tilde{\sigma}_{\alpha\beta}(\mathbf{x}) = \oint_C A_{\alpha\beta ijklm}\partial_i\partial_j\partial_k \left[\int R(\mathbf{x}-\mathbf{x}'')g_m(\mathbf{x}''-\mathbf{x}')\,\mathrm{d}^3\mathbf{x}''\right] \mathrm{d}x'_l, \tag{18}$$

$$\tilde{E} = \oint_C \oint_C B_{ijklmn}\partial_i\partial_j \left[\iint R(\mathbf{x}''-\mathbf{x}''')g_m(\mathbf{x}-\mathbf{x}'')g'_n(\mathbf{x}'-\mathbf{x}''')\,\mathrm{d}^3\mathbf{x}''\,\mathrm{d}^3\mathbf{x}'''\right] \mathrm{d}x_k\,\mathrm{d}x'_l. \tag{19}$$

These expressions reduce to Eqs. (15) and (16) when $\mathbf{g}(\mathbf{x}) = \mathbf{b}\delta^3(\mathbf{x})$ and $\mathbf{g}'(\mathbf{x}) = \mathbf{b}'\delta^3(\mathbf{x})$, where $\delta^3(\mathbf{x})$ is the 3D delta function.

This formulation is rather general and can be used to account for various realistic details of dislocation core structure, e.g. possible splitting of a perfect dislocation into partial dislocations in FCC crystals. However, our purpose here is different: we would like to find $\mathbf{g}(\mathbf{x})$ such that the resulting non-singular solutions are simple and closely resemble the singular solutions of the classical theory. Specifically, consider an isotropic distribution of the form

$$\mathbf{g}(\mathbf{x}) = \mathbf{b}\tilde{w}(\mathbf{x}) = \mathbf{b}\tilde{w}(r), \tag{20}$$

where $r \equiv \|\mathbf{x}\|$. Now, define $w(\mathbf{x})$ as the convolution of $\tilde{w}(\mathbf{x})$ with itself, i.e.,

$$w(\mathbf{x}) \equiv \tilde{w}(\mathbf{x}) * \tilde{w}(\mathbf{x}) \equiv \int \tilde{w}(\mathbf{x}-\mathbf{x}')\tilde{w}(\mathbf{x}')\,\mathrm{d}^3\mathbf{x}'. \tag{21}$$

Obviously, because $\tilde{w}(\mathbf{x})$ is isotropic, $w(\mathbf{x})$ is isotropic as well, i.e. $w(\mathbf{x}) = w(r)$. Defining $R_a(\mathbf{x})$ as the convolution of $R(\mathbf{x})$ with $w(\mathbf{x})$:

$$R_a(\mathbf{x}) \equiv R(\mathbf{x}) * w(\mathbf{x}) \equiv \int R(\mathbf{x}-\mathbf{x}')w(\mathbf{x}')\,\mathrm{d}^3\mathbf{x}' \tag{22}$$

the energy of the dislocation loop becomes

$$\tilde{E} = \oint_C \oint_C B_{ijklmn}\partial_i\partial_j R_a(\mathbf{x}-\mathbf{x}')b_m b'_n\,\mathrm{d}x_k\,\mathrm{d}x'_l. \tag{23}$$

Notice that for $\mathbf{x} = (x, y, z)$, $R(\mathbf{x}) = \sqrt{x^2+y^2+z^2}$, so that the spatial derivatives of R follow some simple rules, e.g.,

$$\frac{\partial R}{\partial x} = \frac{x}{R}, \tag{24}$$

$$\frac{\partial^2 R}{\partial x^2} = \frac{1}{R} - \frac{x^2}{R^3}, \tag{25}$$

$$\frac{\partial^2 R}{\partial x \partial y} = -\frac{xy}{R^3}. \tag{26}$$

Suppose we can find a function $w(\mathbf{x})$ such that

$$R_a(\mathbf{x}) \equiv R(\mathbf{x}) * w(\mathbf{x}) = \sqrt{R(\mathbf{x})^2 + a^2} = \sqrt{x^2+y^2+z^2+a^2}, \tag{27}$$

where a is an arbitrary constant (core width), then the spatial derivatives of R_a follow the same simple rules as those of R, e.g.,

$$\frac{\partial R_a}{\partial x} = \frac{x}{R_a}, \tag{28}$$

$$\frac{\partial^2 R_a}{\partial x^2} = \frac{1}{R_a} - \frac{x^2}{R_a^3}, \tag{29}$$

$$\frac{\partial^2 R_a}{\partial x \partial y} = -\frac{xy}{R_a^3}. \tag{30}$$

As long as $a > 0$, derivatives $\partial_i\partial_j R_a$ are non-singular and their expressions are similar to $\partial_i\partial_j R$. The energy of a dislocation spread in this specific fashion is finite while its expression closely resembles that of the classical singular solution (with $a = 0$). For example, the energy of a closed loop C the energy is given by the following double integral:

$$\begin{aligned} E^{\mathrm{ns}} = & -\frac{\mu}{8\pi}\oint_C\oint_C \partial_k\partial_k R_a b_i b'_j\,\mathrm{d}x_i\,\mathrm{d}x'_j - \frac{\mu}{4\pi(1-\nu)}\oint_C\oint_C \partial_i\partial_j R_a b_i b'_j\,\mathrm{d}x_k\,\mathrm{d}x'_k \\ & + \frac{\mu}{4\pi(1-\nu)}\left[\oint_C\oint_C \partial_k\partial_k R_a b_i b'_i\,\mathrm{d}x_j\,\mathrm{d}x'_j - \nu\oint_C\oint_C \partial_k\partial_k R_a b_i b'_j\,\mathrm{d}x_j\,\mathrm{d}x'_i\right]. \end{aligned} \tag{31}$$

We note that our approach does not share the artifact of the regularization Approach I described in Section 3, because a closed dislocation loop remains closed after spreading it out. Therefore, the non-singular dislocation energy would not change if one were to use a different form of the integrand in the above expressions (Blin, 1995; de Wit, 1960, 1967a, b).

The function $w(\mathbf{x})$ that leads to $R_a = \sqrt{R^2 + a^2}$ is (see Appendix A)

$$w(\mathbf{x}) = \frac{15}{8\pi a^3[(r/a)^2 + 1]^{7/2}}, \quad r = \|\mathbf{x}\|. \tag{32}$$

Notice that $w(\mathbf{x})$ is the convolution of the Burgers vector distribution function $\tilde{w}(\mathbf{x})$ with itself (Eq. (21)). From Eq. (32), $\tilde{w}(\mathbf{x})$ can also be obtained (see Appendix A). $\tilde{w}(r)$ and $w(r)$ are plotted in Figs. 3(a) and (b).

The non-singular stress field $\tilde{\sigma}_{\alpha\beta}$ produced by the dislocation at point $\mathbf{x}$ is given by Eq. (18). However, it will be inconsistent to simply plug this stress into the Peach–Koehler equation to get the local force on another distributed dislocation centered at point $\mathbf{x}$. When the latter dislocation is spread at point $\mathbf{x}$ according to the same distribution $\tilde{w}(\mathbf{x})$, the force at this point is obtained by a second convolution $\tilde{\sigma}_{\alpha\beta}(\mathbf{x})$ with $\tilde{w}(\mathbf{x})$. In this case, a more relevant measure of local stress field is

$$\begin{aligned}\sigma^{\mathrm{ns}}_{\alpha\beta}(\mathbf{x}) &\equiv \tilde{\sigma}_{\alpha\beta}(\mathbf{x}) * \tilde{w}(\mathbf{x}) \\ &= \frac{\mu}{8\pi}\oint_C \partial_i\partial_p\partial_p R_a[b_m\varepsilon_{im\alpha}\,\mathrm{d}x'_\beta + b_m\varepsilon_{im\beta}\,\mathrm{d}x'_\alpha] \\ &\quad + \frac{\mu}{4\pi(1-\nu)}\oint_C b_m\varepsilon_{imk}(\partial_i\partial_\alpha\partial_\beta R_a - \delta_{\alpha\beta}\partial_i\partial_p\partial_p R_a)\,\mathrm{d}x'_k.\end{aligned} \tag{33}$$

The driving force $\mathbf{f}^{\mathrm{ns}}$ on a dislocation with isotropically distributed dislocation core centered about a point $\mathbf{x}$ is related to this "non-singular" stress $\sigma^{\mathrm{ns}}_{\alpha\beta}(\mathbf{x})$ through the Peach–Koehler formula

$$\mathbf{f}^{\mathrm{ns}}_i(\mathbf{x}) = \varepsilon_{ijk}b_l\xi_k\sigma^{\mathrm{ns}}_{jl}(\mathbf{x}). \tag{34}$$

The physical interpretation of $\sigma^{\mathrm{ns}}_{\alpha\beta}(\mathbf{x})$ (apart from its relation with $\mathbf{f}^{\mathrm{ns}}$) is that it is the convolution of the stress at field point $\mathbf{x}$ with the same function $\tilde{w}(\mathbf{x})$ that defines the spreading of the "source" dislocation core; it is the stress field to use for computing

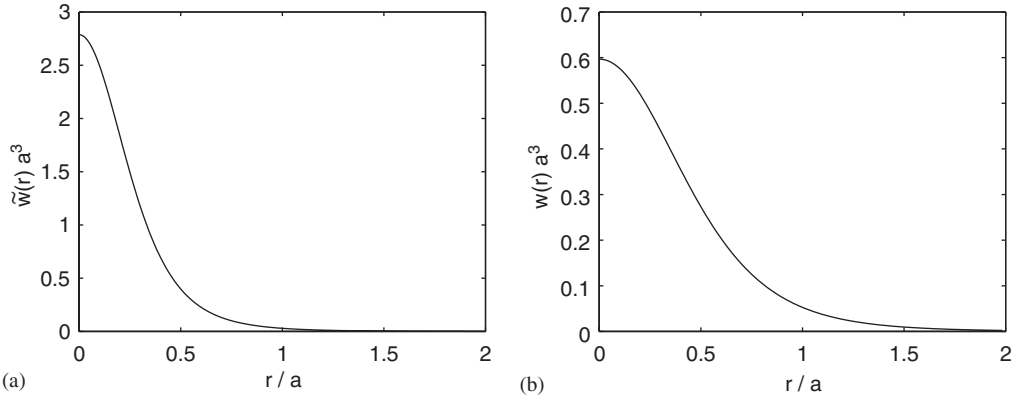

Fig. 3. (a) Burgers vector distribution function $\tilde{w}(r) = \tilde{w}(\mathbf{x})$ where $r = \|\mathbf{x}\|$. (b) $w(r) = w(\mathbf{x}) = \tilde{w}(\mathbf{x}) * \tilde{w}(\mathbf{x})$.

the Peach–Koehler force on the dislocations. In other situations, it can be of interest to compute stress $\tilde{\sigma}_{\alpha\beta}(\mathbf{x})$ of a "source" dislocation at field point $\mathbf{x}$ that is not convoluted with function $\tilde{w}(\mathbf{x})$ for the second time. Given that function $\tilde{w}(\mathbf{x})$ can be well approximated by linear combinations of functions $w(\mathbf{x})$ (see Appendix A), the above expressions for $\sigma^{\mathrm{ns}}_{\alpha\beta}(\mathbf{x})$ can also be used to construct an accurate approximation for $\tilde{\sigma}_{\alpha\beta}(\mathbf{x})$. In any case, when point $\mathbf{x}$ is far away from the "source" dislocation (compared with spread radius a), the difference between $\tilde{\sigma}_{\alpha\beta}(\mathbf{x})$ and $\sigma^{\mathrm{ns}}_{\alpha\beta}(\mathbf{x})$ becomes vanishingly small.

5. Non-singular stress and energy: analytical results

This section considers several simple dislocation geometries for which close form analytic solutions can be found. Our primary purpose here is to present the non-singular solutions and compare them to their counterparts in the classical theory. All expressions presented below are non-singular for $a>0$ and reduce to the classical singular solutions when $a \to 0$. Somewhat more complicated expressions for the stress field of a straight dislocation segment are given in Appendix B, both in a coordinate-dependent and in a coordinate-independent (dyadic) forms. Analytic solutions for the self-energy of a straight dislocation segment and the interaction energy of two straight dislocation segments are given in Appendix C, in the coordinate-independent form only. Suitable for DD simulations, these solutions have been implemented into MATLAB and can be downloaded from our website (Cai and Arsenlis, 2005).

5.1. Stress of an infinite straight screw dislocation

For an infinite straight screw dislocation along z axis, with $b_x = b_y = 0$, $b_z = b$, the non-singular solution for the stress field is

$$\sigma^{\mathrm{ns}}_{xz} = -\frac{\mu b}{2\pi}\frac{y}{\rho_a^2}\left(1+\frac{a^2}{\rho_a^2}\right), \tag{35}$$

$$\sigma^{\mathrm{ns}}_{yz} = \frac{\mu b}{2\pi}\frac{x}{\rho_a^2}\left(1+\frac{a^2}{\rho_a^2}\right), \tag{36}$$

$$\sigma^{\mathrm{ns}}_{xx} = \sigma^{\mathrm{ns}}_{yy} = \sigma^{\mathrm{ns}}_{zz} = \sigma^{\mathrm{ns}}_{xy} = 0, \tag{37}$$

where $\rho_a = \sqrt{x^2+y^2+a^2}$. In polar coordinates, the only non-zero stress component is

$$\sigma^{\mathrm{ns}}_{\theta z} = \frac{\mu b}{2\pi}\frac{r}{\rho_a^2}\left(1+\frac{a^2}{\rho_a^2}\right), \tag{38}$$

where $r = \sqrt{x^2+y^2}$. Comparing these solutions to the classical singular solutions, it is immediately apparent that as $a \to 0$ the classical solutions are recovered.

5.2. Stress of an infinite straight edge dislocation

For an edge dislocation along z axis, with $b_x = b$, $b_y = b_z = 0$, the non-singular solution is

$$\sigma^{\mathrm{ns}}_{xx} = -\frac{\mu b}{2\pi(1-\nu)}\frac{y}{\rho_a^2}\left[1+\frac{2(x^2+a^2)}{\rho_a^2}\right],$$

$$\sigma_{yy}^{\mathrm{ns}} = \frac{\mu b}{2\pi(1-\nu)}\frac{y}{\rho_a^2}\left[1-\frac{2(y^2+a^2)}{\rho_a^2}\right],$$

$$\sigma_{zz}^{\mathrm{ns}} = -\frac{\mu b\nu}{\pi(1-\nu)}\frac{y}{\rho_a^2}\left[1+\frac{a^2}{\rho_a^2}\right],$$

$$\sigma_{xy}^{\mathrm{ns}} = \frac{\mu b}{2\pi(1-\nu)}\frac{x}{\rho_a^2}\left[1-\frac{2y^2}{\rho_a^2}\right],$$

$$\sigma_{xz}^{\mathrm{ns}} = \sigma_{yz}^{\mathrm{ns}} = 0. \tag{39}$$

Again, as $a \to 0$, the classical singular solution for the stress field about an infinite straight edge dislocation is recovered.

5.3. Circular dislocation loop

In the case of a circular dislocation loop of radius $\mathscr{R}$ and Burgers vector b in the loop plane, the non-singular solution for the loop's self-energy is

$$W^{\mathrm{GL}} = 2\pi\mathscr{R}\frac{\mu b^2}{8\pi}\left[\frac{2-\nu}{1-\nu}\left(\ln\frac{8\mathscr{R}}{a}-2\right)+\frac{1}{2}\right]+\mathscr{O}\left(\frac{a^2}{\mathscr{R}^2}\right). \tag{40}$$

This should be compared with the singular expression Eqs. (6)–(51) of Hirth and Lothe (1982, p. 169) obtained using a core cut-off r_c, $W = 2\pi\mathscr{R}((2-\nu)/2(1-\nu))(\mu b^2/4\pi)(\ln(4\mathscr{R}/r_c)-2)$. The driving force for change of the loop radius $\mathscr{R}$ (assuming that the loop remains circular) is

$$f_{\mathscr{R}}^{\mathrm{GL}} = -\frac{\mathrm{d}W^{\mathrm{GL}}}{\mathrm{d}\mathscr{R}} = -\frac{\mu b^2}{4}\left[\frac{2-\nu}{1-\nu}\left(\ln\frac{8\mathscr{R}}{a}-1\right)+\frac{1}{2}\right]+\mathscr{O}\left(\frac{a^2}{\mathscr{R}^2}\right). \tag{41}$$

Similarly, for a prismatic dislocation loop of radius $\mathscr{R}$ whose Burgers vector b is perpendicular to the loop plane, the non-singular self-energy is

$$W^{\mathrm{PL}} = 2\pi\mathscr{R}\frac{\mu b^2}{4\pi(1-\nu)}\left(\ln\frac{8\mathscr{R}}{a}-1\right)+\mathscr{O}\left(\frac{a^2}{\mathscr{R}^2}\right). \tag{42}$$

This should be compared with the singular expression Eqs. (6)–(52) of Hirth and Lothe (1982, p. 169) obtained using a core cut-off r_c, $W = 2\pi\mathscr{R}(\mu b^2/4\pi(1-\nu))(\ln(4\mathscr{R}/r_c)-1)$. The driving force for changing the loop radius $\mathscr{R}$ (in this case by climb) is

$$f_{\mathscr{R}}^{\mathrm{PL}} = -\frac{\mathrm{d}W^{\mathrm{PL}}}{\mathrm{d}\mathscr{R}} = -\frac{\mu b^2}{2(1-\nu)}\ln\frac{8\mathscr{R}}{a}+\mathscr{O}\left(\frac{a^2}{\mathscr{R}^2}\right). \tag{43}$$

6. Self-consistency of the non-singular solutions: numerical results

Self-consistency of our non-singular theory can be shown quite generally following the procedure described in Hirth and Lothe (1982, p. 107). However, it is also worthwhile to demonstrate self-consistency numerically. To do so, we calculate the forces two ways, first, as the numerical derivatives of the energy function and, second, through the Peach–Koehler formula. By showing that so-computed forces agree with each other, self-consistency is assured with a bonus of asserting correctness of the numerical

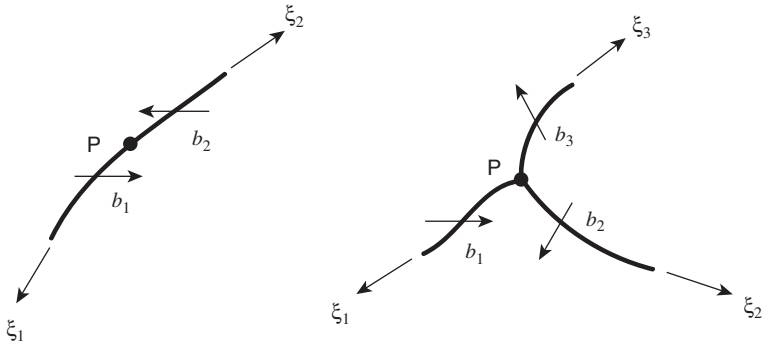

Fig. 4. The Burgers vector is conserved at every point in the dislocation network. This holds true both for "discretization" nodes (on the left) and for "physical" nodes, e.g. the nodes connecting three or more dislocation together (on the right). Following the convention that the line direction $\boldsymbol{\xi}$ always flows out of the node, the Burgers vector conservation can be written as, $\sum_i \mathbf{b}_i = 0$ for every node P in the dislocation network.

implementation of the energy, stress and force expressions. Such self-consistency can only be expected for dislocation configurations in which the Burgers vector is conserved everywhere. In our representation, the degrees of freedom are nodes connected by straight line segments with a constant Burgers vector along each segment. As shown in Fig. 4, Burgers vector conservation requires that the sum of the Burgers vectors at every node must be zero, when the flow directions (sense vectors $\boldsymbol{\xi}$) for all the segments connected to this node are defined outward from the node. We also examine the issue of numerical convergence when a curved dislocation is represented by increasingly fine segments.

6.1. Forces on the nodes

The total energy E^{ns} of a discretized dislocation configuration is calculated by summing up the self-energies and the interaction energies of all its segments, as in Eq. (7). The expressions for the self and interaction energies are given in Appendix C. Now, the force on node i in the discretized system can be found as the minus derivative of the total energy with respect to the node position, i.e.

$$\mathbf{f}_i^{\mathrm{ns}} = -\partial E^{\mathrm{ns}}/\partial \mathbf{r}_i. \tag{44}$$

Alternatively, the force on a node can also be obtained using the virtual force argument, i.e. by computing appropriate line integrals of the Peach–Koehler force over the segments connected to the node. For example, consider the segment $\mathbf{r}_1$–$\mathbf{r}_2$ in Fig. 5. The coordinate system is defined such that $\mathbf{r}_1$ is at the origin and $\mathbf{r}_2$ is a distance $L = \|\mathbf{r}_2 - \mathbf{r}_1\|$ away on the z-axis. The contribution from segment $\mathbf{r}_1$–$\mathbf{r}_2$ to the force on node $\mathbf{r}_2$ is equal to the work of the Peach–Koehler force as the segment sweeps over a triangular shaped area due to a virtual displacement of node at $\mathbf{r}_2$, i.e.,

$$\mathbf{f}_2^{\mathrm{ns}}(1,2) = \int_0^L \frac{z}{L}\mathbf{f}^{\mathrm{ns}}(z)\,\mathrm{d}z, \tag{45}$$

where $\mathbf{f}^{\mathrm{ns}}(z)$ is the Peach–Koehler force per unit length on the segment spanning $z \in [0, L]$. The non-singular Peach–Koehler force is defined in Eq. (34). The total force on a node is then the sum of the partial forces computed in this manner for each segment that it

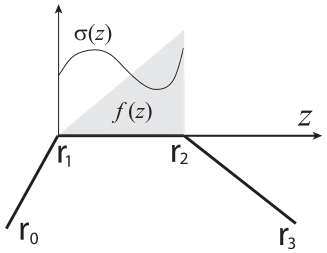

Fig. 5. Computing driving force on node $\mathbf{r}_2$. The contribution from segment $\mathbf{r}_1$–$\mathbf{r}_2$ is the integral $\int_0^L f(z)\sigma(z)\,\mathrm{d}z$, where $f(z) = z$ is the weight function.

connects. In Fig. 5, a similar contribution $\mathbf{f}_2^{\mathrm{ns}}(2,3)$ to the driving force on node $\mathbf{r}_2$, comes from segment $\mathbf{r}_2$–$\mathbf{r}_3$. Thus the total driving force on the node at $\mathbf{r}_2$ is

$$\mathbf{f}_2^{\mathrm{ns}} = \mathbf{f}_2^{\mathrm{ns}}(1,2) + \mathbf{f}_2^{\mathrm{ns}}(2,3). \tag{46}$$

A compact expression for the contribution of a straight dislocation segment to the partial forces on the endpoint nodes of another dislocation segment has been obtained analytically.[2] To conserve space, we do not give these analytical node force expressions in this paper but make them available in a MATLAB implementation on the website (Cai and Arsenlis, 2005). The results presented below were obtained using a DD code written in MATLAB also available from the same website.

6.2. Tests for self-consistency and numerical convergence

Consider a circular dislocation loop with radius $\mathscr{R} = 10$ (in arbitrary units) in the x–y plane: this geometry has been studied extensively in the literature. Set the Burgers vector $\mathbf{b} = [100]$, shear modulus $\mu = 1$, Poisson's ratio $\nu = 0.3$, core width parameter $a = 0.1$ and represent the loop by N nodes connected by straight segments of equal length, as shown in Fig. 6(a). The force on each node of the loop is first computed by numerically differentiating the total energy with respect to the nodal positions. Then, the same nodal forces are obtained by summing up the contributions from the Peach–Koehler forces integrated over the segments, as in Eq. (45). Fig. 6(b) shows that the forces obtained in two different ways agree very well. In fact, the maximum difference between the two forces is less than $10^{-3}\%$ and attributed to the error in the (centered) finite difference scheme used to take numerical derivatives of the total energy. Notice that the discretized geometry contains sharp corners at every node connecting the neighboring straight segments. Our non-singular formulation handles this and other similar situations gracefully, whereas the other existing approaches, e.g. Gavazza and Barnett (1976), require a finite radius of curvature at the point of force evaluation.

Numerical convergence of the total energy and radial force on the loop is illustrated in Fig. 7. Part (a) shows the difference between the loop energy W^{GL} computed numerically and an analytic solution (Eq. (40)), as a function of the number of segments N. Part (b)

[2]We would like to point out that in our implementation, the stress field of a finite straight dislocation segment is generally non-zero on itself. This leads to a non-zero "self" contribution to the forces on the two end nodes of the segment.

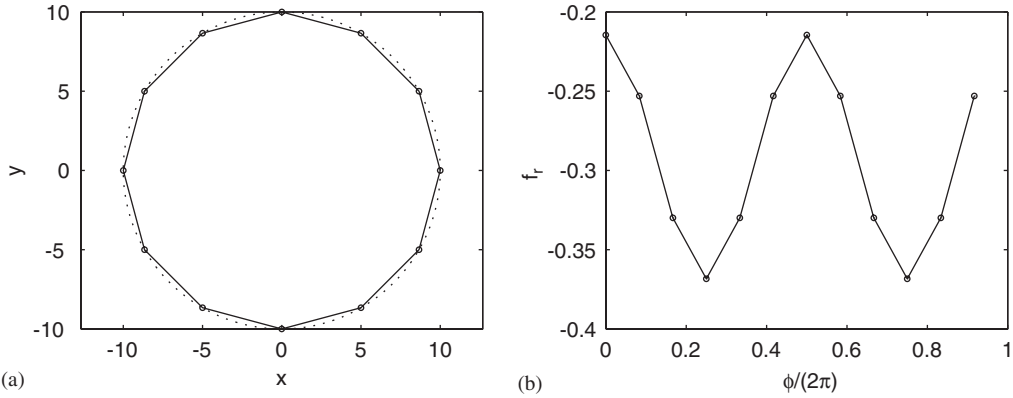

Fig. 6. (a) A circular glide loop (dashed line) in the x–y plane with Burgers vector $\mathbf{b} = [100]$ is discretized into $N = 12$ segments (solid line) connecting N nodes (small open circles). (b) The radial component on nodal force shown here as a function of node (angular) position along the loop. The straight lines are obtained by stress integration over the segments and circles are obtained by numerical differentiation. For every point on the loop, ϕ marks its orientation angle with respect to x-axis.

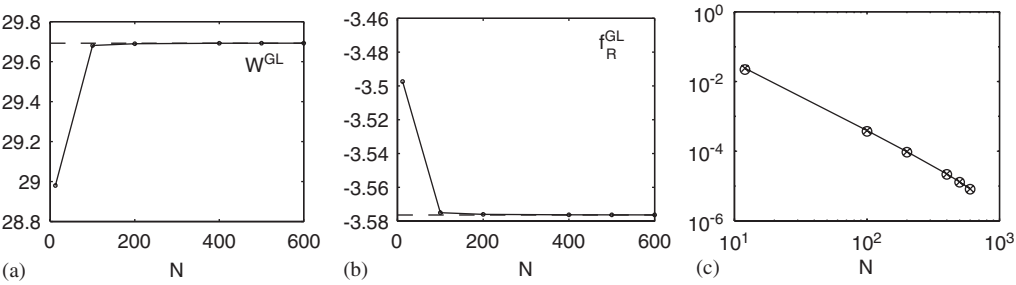

Fig. 7. (a) Elastic energy W^{GL} computed for $N = 12, 100, 200, 400, 500, 600$ (circle), where N is the number of straight segments representing a glide dislocation loop of radius $\mathscr{R}$. The dashed line is the analytic solution Eq. (40) (neglecting the $\mathcal{O}(a^2/\mathscr{R}^2)$ terms). (b) Total radial force summed over all nodes, compared to the analytic solution for $f_{\mathscr{R}}^{\mathrm{GL}} = -\partial W^{\mathrm{GL}}(\mathscr{R})/\partial\mathscr{R}$ given in Eq. (41) (dashed line). (c) (Crosses) The relative deviation of W^{GL} computed for $N = 12, 100, 200, 400, 500, 600$, from the converged numerical value ($N = 1200$). (Circles) The relative deviation of $f_{\mathscr{R}}^{\mathrm{GL}}$ as a function of the number of nodes N.

shows the difference between the radial components of the nodal forces (summed over all N nodes) and the corresponding analytic expression, Eq. (41). The deviation of the numerical results from the analytic solutions at large N is no more than $10^{-2}\%$ in both cases. Part of this slight difference is due to the neglect of $\mathcal{O}(a^2/\mathscr{R}^2)$ terms in the analytic solutions Eqs. (40) and (41). To remove this uncertainty, the numerical results are also compared to the (presumably fully converged) energy and force computed for a very large number of nodes, $N = 1200$ (Fig. 7). The deviation from the limit of large N is seen to decay approximately at a rate of N^{-2}. We would like to note that for the finest discretizations, e.g. $N = 600$ and $N = 1200$, the segment length is about the same as or even smaller than the core width parameter a. Our non-singular theory remains robust for arbitrarily short segments connected at sharp corners.

7. Comparison with a previous model

The difference between this non-singular model and the previous models lies in their different treatments of the dislocation core. Lothe (1992) selected a uniform Burgers vector distribution; Gavazza and Barnett (1976) excluded a tubular region from total energy calculation; and the actual atomic character of the Burgers vector in a real crystal may correspond to yet another Burgers vector distribution. Obviously, different core models can lead to different energy and forces for the same dislocation configuration. Here we intend to show, by comparison to another model, that two continuum approaches based on two different core models can be reconciled by adding an appropriate line energy integral. To avoid possible unwanted effects of non-self-consistent treatment we choose to compare our non-singular self-consistent model with the non-singular self-consistent model of Gavazza and Barnett (1976).

Consider two self-consistent elasticity models that rely on two different treatments of the dislocation core. Let $E^1_{\rm el}(C,a)$ be the elastic energy of a dislocation loop C given by model 1 with a regularization parameter a. Let $E^2_{\rm el}(C,a)$ be the elastic energy of the same loop given by model 2. We now intend to show that, under certain conditions to be specified later, the difference between $E^1_{\rm el}(C,a)$ and $E^2_{\rm el}(C,a)$ can be subsumed into a line integral along the dislocation loop, i.e.,

$$E^2_{\rm el}(C,a) - E^1_{\rm el}(C,a) \approx \int_C E^{2-1}_{\rm core}(\theta,a)\,{\rm d}l, \tag{47}$$

where $E^{2-1}_{\rm core}(\theta,a)$ is an energy difference per unit length of the dislocation. This function can depend on the local character angle θ and on the core parameter a. Notice that because dislocation segments have long range interactions, both $E^1_{\rm el}(C,a)$ and $E^2_{\rm el}(C,a)$ necessarily involve double line integrals over C, such as in Eq. (31). Therefore, Eq. (47) is a non-trivial statement, insisting that the difference between two double line integrals can be well approximated by a single line integral. This limits the range of admissible differences between the predictions of two self-consistent models.

Since Eq. (47) should hold for different dislocation configurations, we should be able to compute the core energy difference by comparing the energies of very simple dislocation configurations. Then, the same core energy function should be able to account for the energy and force differences predicted by the two models in more complex dislocation configurations. As a demonstration, we first obtain the core energy difference function between the Gavazza and Barnett (1976) model and the present model. The simplest structure to extract core energy differences is a dipole of infinitely long parallel dislocations with opposite Burgers vectors. In the isotropic elasticity, the stress and strain fields of edge and screw components of a dislocation dipole do not mix, so that the dipole energy is simply the sum of the energies of its edge and screw components.

In the Gavazza–Barnett model (model 1), the energy (per unit length) of a screw dislocation dipole with Burgers vector b is

$$E^1_{\rm s.d.} = \frac{\mu b^2}{2\pi}\left[\ln\frac{\mathscr{R}}{a} + \mathscr{O}\left(\frac{a}{\mathscr{R}}\right)\right], \tag{48}$$

where $\mathscr{R}$ is the distance between two dislocations of the dipole. Here, without loss of generality, we have chosen the tube radius ρ to be the same as our core width a. The energy (per unit length) of an edge dislocation dipole with Burgers vector b parallel to the

separation vector of the two dislocations is

$$E^1_{\text{e.d.}} = \frac{\mu b^2}{2\pi(1-\nu)}\left[\ln\frac{\mathscr{R}}{a} - \frac{1-2\nu}{4(1-\nu)} + \mathcal{O}\left(\frac{a}{\mathscr{R}}\right)\right]. \tag{49}$$

Now in the present model (model 2), the energy of the screw dislocation dipole is

$$E^2_{\text{s.d.}} = \frac{\mu b^2}{2\pi}\left[\ln\frac{\mathscr{R}}{a} + \frac{1}{2} + \mathcal{O}\left(\frac{a^2}{\mathscr{R}^2}\right)\right]. \tag{50}$$

The energy of the edge dislocation dipole is

$$E^2_{\text{e.d.}} = \frac{\mu b^2}{2\pi(1-\nu)}\left[\ln\frac{\mathscr{R}}{a} + \mathcal{O}\left(\frac{a^2}{\mathscr{R}^2}\right)\right]. \tag{51}$$

The energy difference between the two models for a dislocation dipole with an arbitrary character angle θ is

$$(E^2_{\text{s.d.}} - E^1_{\text{s.d.}})\cos^2\theta + (E^2_{\text{e.d.}} - E^1_{\text{e.d.}})\sin^2\theta = 2E^{2-1}_{\text{core}}(\theta, a) + \mathcal{O}\left(\frac{a}{\mathscr{R}}\right),$$

where

$$E^{2-1}_{\text{core}}(\theta, a) \equiv \cos^2\theta \cdot \frac{\mu b^2}{8\pi} + \sin^2\theta \cdot \frac{\mu b^2(1-2\nu)}{16\pi(1-\nu)^2}. \tag{52}$$

Therefore, the energy difference between two models for an arbitrary dislocation dipole (with character angle θ and separation $\mathscr{R}$) can be described by the core energy function, Eq. (52), up to the order of $\mathcal{O}(a/\mathscr{R})$. This indicates the range of applicability of Eq. (47).

To test whether this core energy function also applies to dislocation structures other than the dipoles, consider a circular glide dislocation loop of radius $\mathscr{R}$. By integrating the above core energy function over the loop, the net core energy difference between two models for this loop would be

$$\int_0^{2\pi} E^{2-1}_{\text{core}}(\theta, a)\mathscr{R}\,\mathrm{d}\theta = \pi\mathscr{R}\left[\frac{\mu b^2}{8\pi} + \frac{\mu b^2(1-2\nu)}{16\pi(1-\nu)^2}\right]. \tag{53}$$

In fact, the elastic energy of this loop by the Gavazza–Barnett model is

$$E^1_{\text{GL}} = 2\pi\mathscr{R}\frac{\mu b^2}{8\pi}\left[\frac{2-\nu}{1-\nu}\left(\ln\frac{8\mathscr{R}}{a} - 2\right) + \frac{-1+2\nu}{4(1-\nu)^2}\right] + \mathcal{O}\left(\frac{a}{\mathscr{R}}\right), \tag{54}$$

while the elastic energy of the same loop by the present model is

$$E^2_{\text{GL}} = 2\pi\mathscr{R}\frac{\mu b^2}{8\pi}\left[\frac{2-\nu}{1-\nu}\left(\ln\frac{8\mathscr{R}}{a} - 2\right) + \frac{1}{2}\right] + \mathcal{O}\left(\frac{a^2}{\mathscr{R}^2}\right). \tag{55}$$

The difference between the E^2_{GL} and E^1_{GL} is exactly given by Eq. (53), up to order of $\mathcal{O}(a/\mathscr{R})$. This agreement confirms that a line energy function exists that matches dislocation total energies obtained within the Gavazza–Barnett model and within our non-singular model.

The core energy difference introduces a difference in the force on the glide loop,

$$f^{2-1}_{\text{core}}(\phi) = \frac{1}{\mathscr{R}}\left[E^{2-1}_{\text{core}}(\phi + \pi/2, a) + \frac{\partial^2}{\partial\phi^2}E^{2-1}_{\text{core}}(\phi + \pi/2, a)\right], \tag{56}$$

where $(\mathscr{R}, \phi)$ is the polar coordinate of a point on the dislocation loop (it is assumed here that the Burgers vector direction is along x-axis, defining the local character angle at every point on the loop as $\theta = \phi + \pi/2$). As shown in Fig. 8, f^{2-1}_{core} accurately accounts for the difference between self-forces along the dislocation loop, as predicted by two models. These results demonstrate consistency between the Gavazza and Barnett (1976) model and the present model, upon the introduction of a core energy function Eq. (52).

The challenge of reconciling our isotropic dislocation core model with more realistic atomic descriptions of dislocations is that the atomic cores are not limited by the assumptions of linear elasticity. However, because the atomistic models are self-consistent by their very nature, we can attempt to account for the difference by a core energy that depends on the local character angle of the dislocation (Cai et al., 2004b). Note that the energy of a given dislocation configuration is defined by the interatomic interactions alone with no reference to any core parameters. On the other hand, the energy defined in our non-singular model depends explicitly on the core width parameter a. Hence, to meaningfully match the atomistic and the non-local elastic predictions for the total energy, the core energy function and the core width parameter a must be specified simultaneously. Even then, consistency is not guaranteed because certain features of the dislocation core in a non-linear and discrete atomistic model cannot be accounted for within continuum linear elasticity.

An accurate way to determine the dislocation core energy is to compute the energy of a dislocation dipole in an atomistic model subject to periodic boundary conditions and to

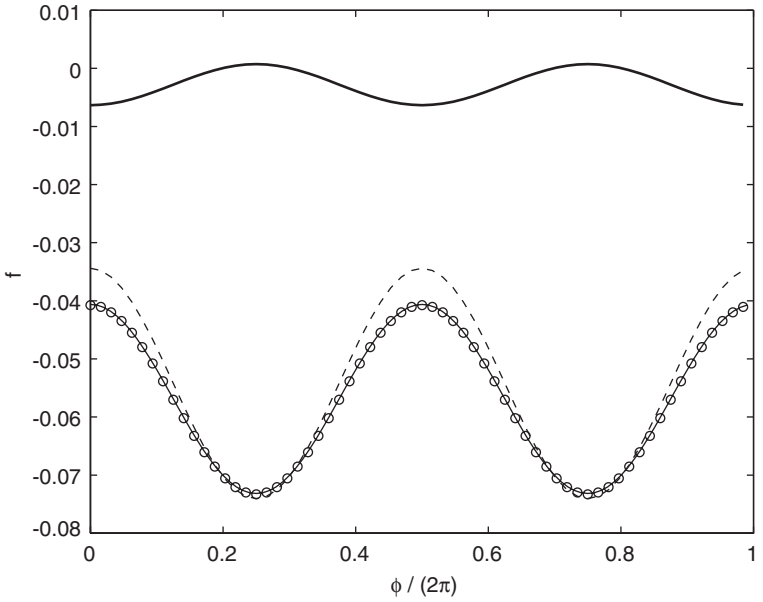

Fig. 8. The radial component of the self-force per unit length on a glide loop with radius $\mathscr{R} = 10$ and regularization parameter $a = 0.1$ ($\mu = 1$, $\nu = 0.3$). Angle ϕ specifies the orientation of a point on the loop with respect to x-axis. The thin solid line: $f^2(\phi)$, the force predicted by the present model. The dashed line: $f^1(\phi)$, the force predicted by the Gavazza–Barnett model. The thick solid line: $f^{2-1}_{\text{core}}(\phi)$, the force difference due to core energy differences predicted by Eq. (56). The circles: the prediction of our model plus the core energy contribution, i.e., $f^1(\phi) + f^{2-1}_{\text{core}}(\phi)$.

compare the result with the energy of the same configuration predicted by the continuum elasticity theory (Cai et al., 2001, 2003). In principle, the core width parameter a in the elastic model can take any value, as long as the core energy is so adjusted that, when added to the elastic energy, it matches the total energy in the atomistic simulation. The choice of the regularization parameter a affects the (artificial) partitioning of the total energy between the "core" energy and "elastic" energy. While a and the core energy term may be arbitrarily chosen to match simple dipole configurations, an arbitrary pair may not necessarily describe the energy of more complex geometries very well. A prudent choice for a is a few Burgers vectors, a typical spread of a dislocation core in an atomistic model. The corresponding core energy function required to match the energy of an atomistic model is typically positive for all character angles.

8. Summary

We presented a self-consistent non-singular theory of dislocations. By allowing the dislocation core to spread according to a carefully chosen isotropic distribution function, non-singular analytic expressions for energy, stress, and forces on the dislocations are obtained. The expressions retain most of the analytic structure of the classical expressions for these quantities but remove the singularity. Our non-singular theory is shown to be self-consistent in that the forces computed from the Peach–Koehler equation and by taking the derivatives of the total energy, agree with each other. Our approach is demonstrated to be consistent with a previous non-singular model, through the introduction of a core energy function. In the same manner, this analytical elasticity theory could be reconciled with more realistic atomistic models of dislocations.

Our method is numerically stable and robust. It is applicable to arbitrary 3D dislocation configurations and has been successfully implemented in two Dislocation Dynamics codes. At the same time, the method remains numerically stable and convergent even when dislocations are represented by very fine line segments. This latter property opens the door to accurate continuum calculations with very high resolution, directly comparable to the atomistic models.

Acknowledgements

The authors wish to thank D.M. Barnett, K.W. Schwarz, M.H. Kalos, J.P. Hirth and L.P. Kubin for useful discussions. The work was performed under the auspices of the U.S. Department of Energy by the University of California, Lawrence Livermore National Laboratory under Contract no. W-7405-Eng-48.

Appendix A. Distribution function $\tilde{w}(r)$ and $w(r)$

First, we prove that $R_a(\mathbf{x}) \equiv R(\mathbf{x}) * w(\mathbf{x}) = [R^2(\mathbf{x}) + a^2]^{1/2}$ when

$$w(\mathbf{x}) = \frac{15}{8\pi a^3[(r/a)^2 + 1]^{7/2}}. \tag{A.1}$$

Taking Laplacian ∇^2 twice on both sides of the equation $R(\mathbf{x}) * w(\mathbf{x}) = R_a(\mathbf{x})$, we obtain

$$\nabla^2[\nabla^2 R(\mathbf{x})] * w(\mathbf{x}) = \nabla^2[\nabla^2 R_a(\mathbf{x})]. \tag{A.2}$$

Because

$$\nabla^2[\nabla^2 R(\mathbf{x})] = \nabla^2\left[\frac{2}{R}\right] = -8\pi\delta^3(\mathbf{x}), \tag{A.3}$$

$$\nabla^2[\nabla^2 R_a(\mathbf{x})] = \nabla^2\left[\frac{2}{R_a} + \frac{a^2}{R_a^3}\right] = -\frac{15a^4}{R_a^7} \tag{A.4}$$

we arrive at

$$w(\mathbf{x}) = \frac{15a^4}{8\pi R_a^7} = \frac{15a^4}{8\pi(r^2+a^2)^{7/2}}. \tag{A.5}$$

This proves Eq. (A.1). Obviously, $w(\mathbf{x}) \to \delta^3(\mathbf{x})$ in the limit $a \to 0$.

Given $w(\mathbf{x})$, $\tilde{w}(\mathbf{x})$ can be obtained numerically by Fourier transform. Specifically, let $W(\mathbf{k})$ and $\tilde{W}(\mathbf{k})$ be the Fourier transforms of $w(\mathbf{x})$ and $\tilde{w}(\mathbf{x})$, respectively. Then $\tilde{W}(\mathbf{k}) = \sqrt{W(\mathbf{k})}$. Obtained by an inverse Fourier transform, the numerical result for $\tilde{w}(\mathbf{x})$ is plotted in Fig. 3(a).

That the single convolution function $\tilde{w}(\mathbf{x})$ is not available in an analytic form is not a limitation when it comes to computing forces on dislocation lines. This is because we intentionally constructed the theory so that what enters the relevant expressions is the double convolution function $w(\mathbf{x})$ that is available in an analytic form. However, if a true (not smeared) stress in a material point is of interest, e.g. for computing the effect of dislocations on a point defect or a grain boundary, we offer the following approximate but "practically" acceptable solution for the single convolution function $\tilde{w}(\mathbf{x})$.

The following expression fits the numerically computed $\tilde{w}(\mathbf{x})$ shown in Fig. 3(a), with a relative error not exceeding 2×10^{-3}:

$$\tilde{w} = \frac{15}{8\pi} \times \left[\frac{1-m}{a_1^3\left(r^2/a_1^2+1\right)^{7/2}} + \frac{m}{a_2^3\left(r^2/a_2^2+1\right)^{7/2}}\right], \tag{A.6}$$

where $a_1 = 0.9038a$, $a_2 = 0.5451a$ and $m = 0.6575$. This function is made up of two functions of the same form as the double convolution function $w(\mathbf{x})$ but with two different (smaller) widths a_1 and a_2. Furthermore, to maintain normalization, the two component functions are weighted with factors $1-m$ and m, respectively. In addition to being nearly exact numerically, this function is convenient to use because the convolution of the singular stress expression with function $w(\mathbf{x})$ is available for arbitrary a (Appendix B). To compute the singly convoluted stress at a point $\mathbf{x}$, all one needs to do is to compute the non-singular stress σ^{ns} at point $\mathbf{x}$ twice using two different values of a and then sum them up with their weights.

Appendix B. Stress field of a straight dislocation segment

B.1. A coordinate-dependent form

Following Hirth and Lothe (1982, p. 133), let us choose a coordinate system such that the dislocation segment lies on z axis, from $z' = z_1$ to $z' = z_2$, as shown in Fig. B.1. Stress at point $\mathbf{x}$ can be now obtained by taking the integral in Eq. (33) along z-axis from z_1 to z_2. The result for $\sigma^{\mathrm{ns}}_{\alpha\beta}$ will be expressed as the difference between the values of the indefinite

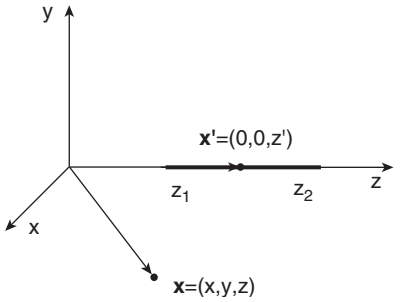

Fig. B.1. A coordinate system for deriving the stress field of a straight dislocation segment.

integral taken at z_1 and z_2,

$$\sigma^{\rm ns}_{\alpha\beta} = \sigma^{\rm ns}_{\alpha\beta}(z' = z_2) - \sigma^{\rm ns}_{\alpha\beta}(z' = z_1). \tag{B.1}$$

Defining

$$\sigma_0 \equiv \frac{\mu}{4\pi(1-\nu)}, \tag{B.2}$$

$$\lambda \equiv z' - z \tag{B.3}$$

the stress components are

$$\frac{\sigma^{\rm ns}_{xx}}{\sigma_0} = \frac{b_x y}{R_a(R_a+\lambda)}\left[1 + \frac{x^2+a^2}{(R_a)^2} + \frac{x^2+a^2}{R_a(R_a+\lambda)}\right] + \frac{b_y x}{R_a(R_a+\lambda)}\left[1 - \frac{x^2+a^2}{(R_a)^2} - \frac{x^2+a^2}{R_a(R_a+\lambda)}\right],$$

$$\frac{\sigma^{\rm ns}_{yy}}{\sigma_0} = \frac{-b_x y}{R_a(R_a+\lambda)}\left[1 - \frac{y^2+a^2}{(R_a)^2} - \frac{y^2+a^2}{R_a(R_a+\lambda)}\right] - \frac{b_y x}{R_a(R_a+\lambda)}\left[1 + \frac{y^2+a^2}{(R_a)^2} + \frac{y^2+a^2}{R_a(R_a+\lambda)}\right],$$

$$\frac{\sigma^{\rm ns}_{zz}}{\sigma_0} = b_x\left\{\frac{2\nu y}{R_a(R_a+\lambda)}\left[1 + \frac{a^2/2}{(R_a)^2} + \frac{a^2/2}{R_a(R_a+\lambda)}\right] + \frac{y\lambda}{(R_a)^3}\right\} - b_y\left\{\frac{2\nu x}{R_a(R_a+\lambda)}\left[1 + \frac{a^2/2}{(R_a)^2} + \frac{a^2/2}{R_a(R_a+\lambda)}\right] + \frac{x\lambda}{(R_a)^3}\right\},$$

$$\frac{\sigma^{\rm ns}_{xy}}{\sigma_0} = \frac{-b_x x}{R_a(R_a+\lambda)}\left[1 - \frac{y^2}{(R_a)^2} - \frac{y^2}{R_a(R_a+\lambda)}\right] + \frac{b_y y}{R_a(R_a+\lambda)}\left[1 - \frac{x^2}{(R_a)^2} - \frac{x^2}{R_a(R_a+\lambda)}\right],$$

$$\frac{\sigma^{\rm ns}_{xz}}{\sigma_0} = -\frac{b_x xy}{(R_a)^3} + b_y\left[-\frac{\nu}{R_a} + \frac{x^2}{(R_a)^3} + (1-\nu)\frac{a^2/2}{(R_a)^3}\right] + \frac{b_z(1-\nu)y}{R_a(R_a+\lambda)}\left[1 + \frac{a^2/2}{(R_a)^2} + \frac{a^2/2}{R_a(R_a+\lambda)}\right],$$

$$\frac{\sigma^{\mathrm{ns}}_{yz}}{\sigma_0} = b_x\left[\frac{v}{R_a} - \frac{y^2}{(R_a)^3} - (1-v)\frac{a^2/2}{(R_a)^3}\right] + b_y\frac{xy}{(R_a)^3} - \frac{b_z(1-v)x}{R_a(R_a+\lambda)}\left[1 + \frac{a^2/2}{(R_a)^2} + \frac{a^2/2}{R_a(R_a+\lambda)}\right]. \tag{B.4}$$

Because the stress can be expressed in several equivalent forms, we will refer to these expressions as *form* 1. In the limit $a \to 0$, $R_a \to R$, and the expressions above reduce to those given in Hirth and Lothe (1982, p. 134). Please note that the above expression cannot be obtained simply by replacing R by R_a in the singular expressions in Hirth and Lothe (1982). For example, there are several terms with a^2 in the numerator which might easily be missed if one takes such a naive approach.

The above expressions (*form* 1) should be used when the field point is to the right of the segment, i.e. $z_1 < z_2 < z$. If, on the other hand, the field point is to the left of the segment, i.e. $z < z_1 < z_2$, then $\lambda < 0$. If, furthermore, the field point is collinear with the segment, i.e. $x = y = 0$, then $R + \lambda = 0$. In the original singular expressions with $a = 0$, *form* 1 is not well behaved numerically in this case, because it contains terms with $R + \lambda$ in the denominator. On the other hand, the stress field itself should be well behaved, since the field point does not overlap with the dislocation segment. The solution is to switch to different stress expressions (*form* 2) that are well behaved in the $z < z_1 < z_2$ regime.

When $a > 0$, this problem never turns up since $R_a + \lambda$ will always be greater than zero. However, it is still a good practice to use *form* 2 when $z < z_1 < z_2$ to preserve the numerical accuracy by avoiding the subtraction of two large numbers to get a small number. *Form* 2 of the stress expressions is given below:

$$\frac{\sigma^{\mathrm{ns}}_{xx}}{\sigma_0} = \frac{-b_x y}{R_a(R_a-\lambda)}\left[1 + \frac{x^2+a^2}{(R_a)^2} + \frac{x^2+a^2}{R_a(R_a-\lambda)}\right] - \frac{b_y x}{R_a(R_a-\lambda)}\left[1 - \frac{x^2+a^2}{(R_a)^2} - \frac{x^2+a^2}{R_a(R_a-\lambda)}\right],$$

$$\frac{\sigma^{\mathrm{ns}}_{yy}}{\sigma_0} = b_x\frac{y\lambda}{\rho_a^2 R_a}\left[1 - \frac{2(y^2+a^2)}{\rho_a^2} - \frac{y^2+a^2}{(R_a)^2}\right] + b_y\frac{x\lambda}{\rho_a^2 R_a}\left[1 + \frac{2(y^2+a^2)}{\rho_a^2} + \frac{y^2+a^2}{(R_a)^2}\right],$$

$$\frac{\sigma^{\mathrm{ns}}_{zz}}{\sigma_0} = b_x\left\{\frac{-2vy}{R_a(R_a-\lambda)}\left[1 + \frac{a^2/2}{(R_a)^2} + \frac{a^2/2}{R_a(R_a-\lambda)}\right] + \frac{y\lambda}{(R_a)^3}\right\} - b_y\left\{\frac{-2vx}{R_a(R_a-\lambda)}\left[1 + \frac{a^2/2}{(R_a)^2} + \frac{a^2/2}{R_a(R_a-\lambda)}\right] + \frac{x\lambda}{(R_a)^3}\right\},$$

$$\frac{\sigma^{\mathrm{ns}}_{xy}}{\sigma_0} = \frac{b_x x}{R_a(R_a-\lambda)}\left[1 - \frac{y^2}{(R_a)^2} - \frac{y^2}{R_a(R_a-\lambda)}\right] - \frac{b_y y}{R_a(R_a-\lambda)}\left[1 - \frac{x^2}{(R_a)^2} - \frac{x^2}{R_a(R_a-\lambda)}\right],$$

$$\frac{\sigma^{\mathrm{ns}}_{xz}}{\sigma_0} = -\frac{b_x xy}{(R_a)^3} + b_y\left[-\frac{v}{R_a} + \frac{x^2}{(R_a)^3} + (1-v)\frac{a^2/2}{(R_a)^3}\right] - \frac{b_z(1-v)y}{R_a(R_a-\lambda)}\left[1 + \frac{a^2/2}{(R_a)^2} + \frac{a^2/2}{R_a(R_a-\lambda)}\right],$$

$$\frac{\sigma_{yz}^{\mathrm{ns}}}{\sigma_0}=\left[\frac{v}{R_a}-\frac{y^2}{(R_a)^3}-(1-v)\frac{a^2/2}{(R_a)^3}\right]+b_y\frac{xy}{(R_a)^3}+\frac{b_z(1-v)x}{R_a(R_a-\lambda)}\left[1+\frac{a^2/2}{(R_a)^2}+\frac{a^2/2}{R_a(R_a-\lambda)}\right]. \tag{B.5}$$

When the field point is between two endpoints of the segment, i.e., $z_1\leqslant z\leqslant z_2$, the following *form* 3 should be used:

$$\frac{\sigma_{xx}^{\mathrm{ns}}}{\sigma_0}=-\frac{b_x y\lambda}{\rho_a^2 R_a}\left[1+\frac{2(x^2+a^2)}{\rho_a^2}+\frac{x^2+a^2}{(R_a)^2}\right]-\frac{b_y x\lambda}{\rho_a^2 R_a}\left[1-\frac{2(x^2+a^2)}{\rho_a^2}-\frac{x^2+a^2}{(R_a)^2}\right],$$

$$\frac{\sigma_{yy}^{\mathrm{ns}}}{\sigma_0}=\frac{b_x y\lambda}{\rho_a^2 R_a}\left[1-\frac{2(y^2+a^2)}{\rho_a^2}-\frac{y^2+a^2}{(R_a)^2}\right]+\frac{b_y x\lambda}{\rho_a^2 R_a}\left[1+\frac{2(y^2+a^2)}{\rho_a^2}+\frac{y^2+a^2}{(R_a)^2}\right],$$

$$\frac{\sigma_{zz}^{\mathrm{ns}}}{\sigma_0}=b_x\left\{\frac{-2vy\lambda}{\rho_a^2 R_a}\left[1+\frac{a^2}{\rho_a^2}+\frac{a^2/2}{(R_a)^2}\right]+\frac{y\lambda}{(R_a)^3}\right\}-b_y\left\{\frac{-2vx\lambda}{\rho_a^2 R_a}\left[1+\frac{a^2}{\rho_a^2}+\frac{a^2/2}{(R_a)^2}\right]+\frac{x\lambda}{(R_a)^3}\right\},$$

$$\frac{\sigma_{xy}^{\mathrm{ns}}}{\sigma_0}=\frac{b_x x\lambda}{\rho_a^2 R_a}\left[1-\frac{2y^2}{\rho_a^2}-\frac{y^2}{(R_a)^2}\right]-\frac{b_y y\lambda}{\rho_a^2 R_a}\left[1-\frac{2x^2}{\rho_a^2}-\frac{x^2}{(R_a)^2}\right],$$

$$\frac{\sigma_{xz}^{\mathrm{ns}}}{\sigma_0}=-\frac{b_x xy}{(R_a)^3}+b_y\left[-\frac{v}{R_a}+\frac{x^2}{(R_a)^3}+(1-v)\frac{a^2/2}{(R_a)^3}\right]-\frac{b_z(1-v)y\lambda}{\rho_a^2 R_a}\left[1+\frac{a^2}{\rho_a^2}+\frac{a^2/2}{(R_a)^2}\right],$$

$$\frac{\sigma_{yz}^{\mathrm{ns}}}{\sigma_0}=b_x\left[\frac{v}{R_a}-\frac{y^2}{(R_a)^3}-(1-v)\frac{a^2/2}{(R_a)^3}\right]+b_y\frac{xy}{(R_a)^3}+\frac{b_z(1-v)x\lambda}{\rho_a^2 R_a}\left[1+\frac{a^2}{\rho_a^2}+\frac{a^2/2}{(R_a)^2}\right]. \tag{B.6}$$

Here $\rho_a\equiv\sqrt{x^2+y^2+a^2}$ and $R_a=\sqrt{x^2+y^2+z^2+a^2}$.

All three forms above are very similar to the original expressions given in Hirth and Lothe (1982). Hence, modifications required to implement the non-singular expressions in place of the singular solutions are minor.

B.2. A coordinate-independent form

Consider a straight dislocation segment with two ends $\mathbf{x}_1$ and $\mathbf{x}_2$ and the Burgers vector $\mathbf{b}$. The stress field of this segment at point $\mathbf{x}$ is

$$\sigma_{ij}^{\mathrm{ns}}(\mathbf{x})=\frac{\mu}{8\pi}\int_{\mathbf{x}_1}^{\mathbf{x}_2}\partial_l\partial_p\partial_p R_a b_k(\varepsilon_{ilk}\,\mathrm{d}x_j'+\varepsilon_{jlk}\,\mathrm{d}x_i')+\frac{\mu}{4\pi(1-v)}\int_{\mathbf{x}_1}^{\mathbf{x}_2}b_k\varepsilon_{lkm}(\partial_l\partial_i\partial_j R_a-\delta_{ij}\partial_l\partial_p\partial_p R_a)\,\mathrm{d}x_m', \tag{B.7}$$

where

$$R_a=\sqrt{(x_k-x_k')(x_k-x_k')+a^2}. \tag{B.8}$$

The result of this integral can be written as

$$\boldsymbol{\sigma}^{\mathrm{ns}}(\mathbf{x}) = \mathbf{T}(\mathbf{x}-\mathbf{x}_2) - \mathbf{T}(\mathbf{x}-\mathbf{x}_1), \tag{B.9}$$

where function $\mathbf{T}$ is defined as

$$\begin{aligned}\frac{\mathbf{T}(\mathbf{R})}{T_o} = {} & [(\mathbf{R}\times\mathbf{b})\cdot\mathbf{t}][A_1(\mathbf{R}\otimes\mathbf{R}) + A_2(\mathbf{t}\otimes\mathbf{R} + \mathbf{R}\otimes\mathbf{t}) + A_3(\mathbf{t}\otimes\mathbf{t}) + A_4\mathbf{I}] \\ & + A_5[(\mathbf{R}\times\mathbf{b})\otimes\mathbf{t} + \mathbf{t}\otimes(\mathbf{R}\times\mathbf{b})] + A_6[(\mathbf{t}\times\mathbf{b})\otimes\mathbf{R} + \mathbf{R}\otimes(\mathbf{t}\times\mathbf{b})] \\ & + A_7[(\mathbf{t}\times\mathbf{b})\otimes\mathbf{t} + \mathbf{t}\otimes(\mathbf{t}\times\mathbf{b})]\end{aligned} \tag{B.10}$$

with

$$T_o = \frac{\mu}{4\pi(1-\nu)}, \tag{B.11}$$

$$\mathbf{t} = \frac{\mathbf{x}_2 - \mathbf{x}_1}{\|\mathbf{x}_2 - \mathbf{x}_1\|}, \tag{B.12}$$

$$A_1 = -\frac{\mathbf{R}\cdot\mathbf{t}[3(R_a)^2 - (\mathbf{R}\cdot\mathbf{t})^2]}{((R_a)^2 - (\mathbf{R}\cdot\mathbf{t})^2)^2(R_a)^3}, \tag{B.13}$$

$$A_2 = \frac{1}{(R_a)^3} - (\mathbf{R}\cdot\mathbf{t})A_1, \tag{B.14}$$

$$A_6 = -\frac{\mathbf{R}\cdot\mathbf{t}}{((R_a)^2 - (\mathbf{R}\cdot\mathbf{t})^2)R_a}, \tag{B.15}$$

$$A_3 = -\frac{\mathbf{R}\cdot\mathbf{t}}{(R_a)^3} + A_6 + (\mathbf{R}\cdot\mathbf{t})^2 A_1, \tag{B.16}$$

$$A_4 = A_6 + a^2 A_1, \tag{B.17}$$

$$A_5 = (\nu-1)A_6 - \frac{a^2(1-\nu)}{2}A_1, \tag{B.18}$$

$$A_7 = \frac{\nu}{R_a} - (\mathbf{R}\cdot\mathbf{t})A_6 - \frac{a^2(1-\nu)}{2}A_2 \tag{B.19}$$

and $\mathbf{I}$ is the identity tensor.

Appendix C. Expressions for self-energies and interaction energies of straight segments

Consider two straight dislocation segments: one segments with its ends at $\mathbf{x}_1$ to $\mathbf{x}_2$ and with Burgers vector $\mathbf{b}$ and another one with its ends at $\mathbf{x}_3$ to $\mathbf{x}_4$ and with Burgers vector $\mathbf{b}'$.

The interaction energy between the two dislocation segments is

$$W^{\mathrm{ns}} = -\frac{\mu}{8\pi}\int_{\mathbf{x}_3}^{\mathbf{x}_4}\int_{\mathbf{x}_1}^{\mathbf{x}_2}\partial_k\partial_k R_a b_i b'_j \,\mathrm{d}x_i\,\mathrm{d}x'_j - \frac{\mu}{4\pi(1-\nu)}\int_{\mathbf{x}_3}^{\mathbf{x}_4}\int_{\mathbf{x}_1}^{\mathbf{x}_2}\partial_i\partial_j R_a b_i b'_j \,\mathrm{d}x_k\,\mathrm{d}x'_k + \frac{\mu}{4\pi(1-\nu)}\left(\int_{\mathbf{x}_3}^{\mathbf{x}_4}\int_{\mathbf{x}_1}^{\mathbf{x}_2}\partial_k\partial_k R_a b_i b'_i \,\mathrm{d}x_j\,\mathrm{d}x'_j - \nu\int_{\mathbf{x}_3}^{\mathbf{x}_4}\int_{\mathbf{x}_1}^{\mathbf{x}_2}\partial_k\partial_k R_a b_i b'_j \,\mathrm{d}x_j\,\mathrm{d}x'_i\right).$$

C.1. Interaction energy between two non-parallel segments

When the two segments are not parallel, their interaction energy can be written as

$$W^{\mathrm{ns}}_{12} = W^{\mathrm{ns}}(\mathbf{x}_4-\mathbf{x}_2) + W^{\mathrm{ns}}(\mathbf{x}_3-\mathbf{x}_1) - W^{\mathrm{ns}}(\mathbf{x}_4-\mathbf{x}_1) - W^{\mathrm{ns}}(\mathbf{x}_3-\mathbf{x}_2). \tag{C.1}$$

The function $W(\cdot)$ is defined as

$$\begin{aligned}\frac{W^{\mathrm{ns}}(\mathbf{R})}{W_o} &= (A_1-A'_2)\mathbf{R}\cdot\mathbf{v}'\ln[R_a+\mathbf{R}\cdot\mathbf{t}'] + A'_3\mathbf{R}\cdot\mathbf{u}\ln[R_a+\mathbf{R}\cdot\mathbf{t}'] \\ &\quad + (A_1-A_2)\mathbf{R}\cdot\mathbf{v}\ln[R_a+\mathbf{R}\cdot\mathbf{t}] + A_3\mathbf{R}\cdot\mathbf{u}\ln[R_a+\mathbf{R}\cdot\mathbf{t}] + A_4R_a \\ &\quad + \frac{(A_1-A_5)[2(\mathbf{R}\cdot\mathbf{u})^2+(\mathbf{u}\cdot\mathbf{u})a^2]}{\sqrt{(\mathbf{u}\cdot\mathbf{u})a^2+(\mathbf{R}\cdot\mathbf{u})^2}}\tan^{-1}\left[\frac{(1+\mathbf{t}\cdot\mathbf{t}')R_a+\mathbf{R}\cdot(\mathbf{t}+\mathbf{t}')}{\sqrt{(\mathbf{u}\cdot\mathbf{u})a^2+(\mathbf{R}\cdot\mathbf{u})^2}}\right],\end{aligned} \tag{C.2}$$

where

$$\mathbf{t} = \frac{\mathbf{x}_2-\mathbf{x}_1}{\|\mathbf{x}_2-\mathbf{x}_1\|}, \tag{C.3}$$

$$\mathbf{t}' = \frac{\mathbf{x}_4-\mathbf{x}_3}{\|\mathbf{x}_4-\mathbf{x}_3\|}, \tag{C.4}$$

$$\mathbf{u} = \mathbf{t}\times\mathbf{t}', \tag{C.5}$$

$$\mathbf{v} = \mathbf{u}\times\mathbf{t}, \tag{C.6}$$

$$\mathbf{v}' = \mathbf{t}'\times\mathbf{u}, \tag{C.7}$$

$$R_a = \sqrt{\mathbf{R}\cdot\mathbf{R}+a^2}, \tag{C.8}$$

$$W_o = \frac{\mu}{4\pi(1-\nu)(\mathbf{u}\cdot\mathbf{u})}, \tag{C.9}$$

$$A_1 = (1-\nu)(\mathbf{b}\cdot\mathbf{t})(\mathbf{b}'\cdot\mathbf{t}') + 2\nu(\mathbf{b}'\cdot\mathbf{t})(\mathbf{b}\cdot\mathbf{t}'), \tag{C.10}$$

$$A_2 = [(\mathbf{b}\cdot\mathbf{b}') + (\mathbf{b}\cdot\mathbf{t})(\mathbf{b}'\cdot\mathbf{t})](\mathbf{t}\cdot\mathbf{t}'), \tag{C.11}$$

$$A'_2 = [(\mathbf{b}\cdot\mathbf{b}') + (\mathbf{b}\cdot\mathbf{t}')(\mathbf{b}'\cdot\mathbf{t}')](\mathbf{t}\cdot\mathbf{t}'), \tag{C.12}$$

$$A'_3 = [(\mathbf{b}\cdot\mathbf{u})(\mathbf{b}'\cdot\mathbf{v}') + (\mathbf{b}'\cdot\mathbf{u})(\mathbf{b}\cdot\mathbf{v}')]\frac{\mathbf{t}\cdot\mathbf{t}'}{\mathbf{u}\cdot\mathbf{u}}, \tag{C.13}$$

$$A_3 = [(\mathbf{b}\cdot\mathbf{u})(\mathbf{b}'\cdot\mathbf{v}) + (\mathbf{b}'\cdot\mathbf{u})(\mathbf{b}\cdot\mathbf{v})]\frac{\mathbf{t}\cdot\mathbf{t}'}{\mathbf{u}\cdot\mathbf{u}}, \tag{C.14}$$

$$A_4 = [(\mathbf{b}\cdot\mathbf{t})(\mathbf{b}'\cdot\mathbf{v}) + (\mathbf{b}\cdot\mathbf{t}')(\mathbf{b}'\cdot\mathbf{v}')](\mathbf{t}\cdot\mathbf{t}'), \tag{C.15}$$

$$A_5 = 2[(\mathbf{b}\times\mathbf{u})\cdot(\mathbf{b}'\times\mathbf{u})]\,\frac{\mathbf{t}\cdot\mathbf{t}'}{\mathbf{u}\cdot\mathbf{u}}. \tag{C.16}$$

C.2. Interaction energy between two parallel segments

When the two segments are parallel, i.e. $\mathbf{t}=\mathbf{t}'$, function $W^{\mathrm{ns}}(\mathbf{R}) = W^{\mathrm{ns}}_{\parallel}(\mathbf{R})$ becomes

$$\frac{W^{\mathrm{ns}}_{\parallel}(\mathbf{R})}{W_o} = \{(\mathbf{b}\cdot\mathbf{t})(\mathbf{b}'\cdot\mathbf{R}) + (\mathbf{b}\cdot\mathbf{R})(\mathbf{b}'\cdot\mathbf{t}) \tag{C.17}$$

$$-[(2-\nu)(\mathbf{b}\cdot\mathbf{t})(\mathbf{b}'\cdot\mathbf{t}) + \mathbf{b}\cdot\mathbf{b}']\mathbf{R}\cdot\mathbf{t}\}\ln[R_a + \mathbf{R}\cdot\mathbf{t}] \tag{C.18}$$

$$+[(1-\nu)(\mathbf{b}\cdot\mathbf{t})(\mathbf{b}'\cdot\mathbf{t}) + \mathbf{b}\cdot\mathbf{b}']R_a \tag{C.19}$$

$$-\frac{[\mathbf{b}\cdot\mathbf{R} - (\mathbf{R}\cdot\mathbf{t})(\mathbf{b}\cdot\mathbf{t})][\mathbf{b}'\cdot\mathbf{R} - (\mathbf{R}\cdot\mathbf{t})(\mathbf{b}'\cdot\mathbf{t})]}{(R_a)^2 - (\mathbf{R}\cdot\mathbf{t})^2}R_a \tag{C.20}$$

$$+\frac{a^2[(1+\nu)(\mathbf{b}\cdot\mathbf{t})(\mathbf{b}'\cdot\mathbf{t}) - 2(\mathbf{b}\cdot\mathbf{b}')]}{2((R_a)^2 - (\mathbf{R}\cdot\mathbf{t})^2)}R_a, \tag{C.21}$$

where

$$W_o = \frac{\mu}{4\pi(1-\nu)}. \tag{C.22}$$

C.3. Self-energy of a dislocation segment

The self-energy of a dislocation segment can be obtained from the solution for the interaction energy of two parallel segments. Since the theory is non-singular, the energy remains finite even when $\mathbf{b}=\mathbf{b}'$, $\mathbf{x}_4=\mathbf{x}_2$, and $\mathbf{x}_3=\mathbf{x}_1$, leading to the following expression for the self-energy:

$$\begin{aligned} W^{\mathrm{ns}}_{\mathrm{self}} &= W^{\mathrm{ns}}_{\parallel}(\mathbf{0}) - W^{\mathrm{ns}}_{\parallel}(\mathbf{x}_2-\mathbf{x}_1) \\ &= \frac{\mu}{4\pi(1-\nu)}\left\{[\mathbf{b}\cdot\mathbf{b} - \nu(\mathbf{b}\cdot\mathbf{t})^2]L\ln\left[\frac{L_a+L}{a}\right] - \frac{3-\nu}{2}(\mathbf{b}\cdot\mathbf{t})^2(L_a-a)\right\}, \end{aligned} \tag{C.23}$$

where

$$L = \|\mathbf{x}_2 - \mathbf{x}_1\|, \tag{C.24}$$

$$L_a = \sqrt{L^2 + a^2}. \tag{C.25}$$

References

Blin, J., 1995. Acta Metall. 3, 199.
Brown, L.M., 1964. The self-stress of dislocations and the shape of extended nodes. Philos. Mag. 10, 441.

Bulatov, V.V., Cai, W., Fier, J., Hiratani, M., Pierce, T., Tang, M., Rhee, M., Yates, K., Arsenlis, A., 2004. Scalable line dynamics of ParaDiS. SuperComputing 19. <http://www.sc-conference.org/sc2004/schedule/pdfs/pap206.pdf>.

Cai, W., 2001. Atomistic and mesoscale modeling of dislocation mobility. Ph.D. Thesis, Massachusetts Institute of Technology.

Cai, W., Arsenlis, A., 2005. MATLAB codes that implement the non-singular stress, energy and force expressions. Available from: <http://micro.stanford.edu/~caiwei/Forum/2005-04-18-NSDD/>.

Cai, W., Bulatov, V.V., Chang, J., Li, J., Yip, S., 2001. Anisotropic elastic interactions of a periodic dislocation array. Phys. Rev. Lett. 86, 5727.

Cai, W., Bulatov, V.V., Chang, J., Li, J., Yip, S., 2003. Periodic image effects in dislocation modelling. Philos. Mag. A 83, 539.

Cai, W., Bulatov, V.V., Pierce, T.G., Hiratani, M., Rhee, M., Bartelt, M., Tang, M., 2004a. Massively-parallel dislocation dynamics simulations. In: Kitagawa, H., Shibutani, Y. (Eds.), Solid Mechanics and Its Applications, vol. 115. Kluwer Academic Publisher, Dordrecht, p. 1.

Cai, W., Bulatov, V.V., Chang, J., Li, J., Yip, S., 2004b. Dislocation core effects on mobility. In: Nabarro, F.R.N., Hirth, J.P. (Eds.), Dislocations in Solids, vol. 12. North-Holland Publishers, Amsterdam, p. 1.

Devincre, B., Kubin, L.P., 1997. Mesoscopic simulations of dislocations and plasticity. Mater. Sci. Eng. A 8, 234–236.

de Wit, R., 1960. Solid State Phys. 10, 249.

de Wit, R., 1967a. Some relations for straight dislocations. Phys. Status Solidi 20, 567.

de Wit, R., 1967b. The self-energy of dislocation configurations made up of straight segments. Phys. Status Solidi 20, 575.

Fedelich, B., 2004. The glide force on a dislocation in finite elasticity. J. Mech. Phys. Solids 52, 215.

Gavazza, S.D., Barnett, D.M., 1976. The self-force on a planar dislocation loop in an anisotropic linear-elastic medium. J. Mech. Phys. Solids 24, 171.

Ghoniem, N.M., Sun, L.Z., 1999. Fast-sum method for the elastic field of three-dimensional dislocation ensembles. Phys. Rev. B 60, 128.

Gutkin, M.Y., Aifantis, E.C., 1996. Screw dislocation in gradient elasticity. Scr. Mater. 35, 1353–1358.

Gutkin, M.Y., Aifantis, E.C., 1997. Edge dislocation in gradient elasticity. Scr. Mater. 36, 129–135.

Hirth, J.P., Lothe, J., 1982. Theory of Dislocations. Wiley, New York.

LeSar, R., 2004. Ambiguities in the calculation of dislocation self energies. Phys. Status Solidi B 241, 2875.

Lothe, J., 1992. In: Indenbohm, V.L., Lothe, J. (Eds.), Elastic Strain Fields and Dislocation Mobility. North-Holland, Amsterdam, p. 182.

Lothe, J., Hirth, J.P., 2005. Dislocation core parameters. Phys. Status Solidi B 242, 836.

Mura, T., 1982. Micromechanics of Defects in Solids. Kluwer, Dordrecht.

Nabarro, F.R.N., 1947. Dislocations in a simple cubic lattice. Proc. Phys. Soc. 59, 256.

Peierls, R.E., 1940. The size of a dislocation. Proc. Phys. Soc. 52, 34.

Schwarz, K.W., 1999. Simulation of dislocations on the mesoscopic scale. I. Methods and examples. J. Appl. Phys. 85, 108.